Developmental Biology 362 (2012) 94–103

Contents lists available at SciVerse ScienceDirect

Developmental Biology

journal homepage: www.elsevier.com/developmentalbiology

EVEN-SKIPPED HOMEOBOX 1 controls human ES cell differentiation by directly repressing *GOOSECOID* expression

Mark Kalisz [a,b], Maria Winzi [a], Hanne Cathrine Bisgaard [b], Palle Serup [a,*]

[a] Department of Developmental Biology, Hagedorn Research Institute, Niels Steensens Vej 6, DK-2820 Gentofte, Denmark
[b] Department of Cellular and Molecular Medicine, Faculty of Health Sciences, University of Copenhagen, Copenhagen, Denmark

ARTICLE INFO

Article history:
Received for publication 20 September 2011
Revised 18 November 2011
Accepted 28 November 2011
Available online 6 December 2011

Keywords:
EVX1
GSC
Brachyury
TGFbeta
Human ES cells

ABSTRACT

TGFß signaling patterns the primitive streak, yet little is known about transcriptional effectors that mediate the cell fate choices during streak-like development in mammalian embryos and in embryonic stem (ES) cells. Here we demonstrate that cross-antagonistic actions of *EVEN-SKIPPED HOMEOBOX 1* (*EVX1*) and *GOOSECOID* (*GSC*) regulate cell fate decisions in streak-like progenitors derived from human ES cells exposed to BMP4 and/or activin. We found that EVX1 repressed *GSC* expression and promoted formation of posterior streak-like progeny in response to BMP4, and conversely that GSC repressed *EVX1* expression and was required for development of anterior streak-like progeny in response to activin. Chromatin immunoprecipitation assays showed that EVX1 bound to the *GSC* 5′-flanking region in BMP4 treated human ES cells, and band shift assays identified two EVX1 binding sites in the *GSC* 5′-region. Significantly, we found that intact EVX1 binding sites were required for BMP4-mediated repression of *GSC* reporter constructs. We conclude that BMP4-induced EVX1 repress GSC directly and the two genes form the core of a gene regulatory network (GRN) controlling cell fates in streak-like human ES cell progeny.

Introduction

Embryonic stem (ES) cells treated with TGFß family members respond much like epiblast cells migrating through the primitive streak (hereafter just the streak) of early vertebrate embryos. High levels of nodal or activin A (hereafter just activin) induce anterior streak and mesendodermal fates while low levels of nodal/activin or BMP4 induce posterior streak and mesodermal fates (D'Amour et al., 2005; Gadue et al., 2006; Hansson et al., 2009; Kubo et al., 2004; Nostro et al., 2008; Tada et al., 2005; Yasunaga et al., 2005). BMP signaling often dominates over nodal/activin signaling when both factors are present. For example, when mouse ES cells (mESC) are treated with high levels of activin in presence of BMP4, activin-induced gene expression is suppressed (Hansson et al., 2009; Nostro et al., 2008), similar to what is seen when treating activin-induced *Xenopus* animal caps with BMP4 (Jones et al., 1996), and consistent with anterior streak development requiring expression of Bmp antagonists such as noggin, chordin, and follistatin (Bachiller et al., 2000; Khokha et al., 2005; Lane et al., 2004; Yang et al., 2010).

In *Xenopus* embryos, three homeobox genes, *Goosecoid* (*Xgsc*), *Vent1/2* and *Xhox3* (acting downstream of *Vent1/2*) form the core of a gene regulatory network (GRN) that patterns the embryo along the anterior–posterior (A–P) axis. *Xgsc* is induced dorsally by nodal while *Vent1/2* and *Xhox3* are induced ventrally by BMP4, and mutual repression between *Xgsc* and the *Vent1/2-Xhox3* "cassette" sets up graded expression of these genes. Loss of *Xgsc* function results in dorsal expansion of Vent1/2 and Xhox3 expression and ventralizes the embryo while loss of *Vent1/2* causes *Xgsc* expression to expand ventrally, loss of *Xhox3* expression, and dorsalization of the embryo (Onichtchouk et al., 1998; Ruiz i Altaba and Melton, 1989a,b; Ruiz i Altaba et al., 1991; Sander et al., 2007; Steinbeisser et al., 1995). Note that the dorsal–ventral axis in pre-gastrula stage amphibian embryos is regarded to be equivalent to the A–P axis of amniote embryos at the streak stage (Keller and Shook, 2008; Lane and Sheets, 2000, 2002, 2006; Lane and Smith, 1999; Lane et al., 2004).

Less is known about the function of these homeobox genes in mammals. Mice do not have an obvious *Vent1/2* ortholog and even though induction of *Gsc* and *Evx1* (the mouse *Xhox3* ortholog) by nodal and Bmp4 is conserved, neither *Gsc* nor *Evx1* knockout mice have overt gastrulation defects (Moran-Rivard et al., 2001; Rivera-Perez et al., 1995; Tada et al., 2005; Yamada et al., 1995; Yasunaga et al., 2005). The human VENTX2 and Xvent2B homeodomains share 65% identity, but the only reported expression is in bone marrow (Moretti et al., 2001) and it is not induced by BMP4 in human ES cells (hESC; this study). Similarly, the function of the human *EVX1* and *GSC* genes in streak development is unknown.

Here we use gain- and loss-of-function experiments to demonstrate that human *EVX1* and *GSC* are required and sufficient to regulate cell fates of induced, streak-like hESC progeny. We found that *EVX1* and *BRACHYURY* (*T*) stimulated each others expression and

* Corresponding author at: Hagedorn Research Institute, Niels Steensens Vej 6, DK-2820, Gentofte, Denmark. Fax: +45 4443 8000.
E-mail address: pas@hagedorn.dk (P. Serup).

0012-1606/$ – see front matter © 2011 Elsevier Inc. All rights reserved.
doi:10.1016/j.ydbio.2011.11.017

promoted development of posterior streak progeny by suppressing *GSC*. We also found that EVX1 and T are required for BMP4 mediated suppression of nodal/activin-induced *GSC* expression and differentiation of SOX17$^+$ definitive endoderm. Chromatin immunoprecipitation (ChIP) showed that EVX1 bound to the *GSC* 5′-flanking region in hESC chromatin in a BMP4-dependent manner, and band shift assays identified two functional EVX1 binding sites in the human *GSC* 5′-region. Reporter assays demonstrated that both EVX1 binding sites were required for efficient BMP4-mediated repression of activin-induced *GSC* expression. Together our results demonstrate that BMP4-induced EVX1 directly repress GSC expression and suggest that mutually repressive interactions between GSC and EVX1 execute nodal and BMP mediated patterning of hESC-derived streak-like progeny.

Materials and methods

Cell culture and differentiation

The hESC lines, H9 (from Wicell, Madison, WI) and SHEF3 (from Sheffield University, Sheffield, UK) were cultured as previously described (Zhang et al., 2008). For differentiation, hESC were seeded at 25000 cells/cm^2 on culture plates (Nunc) coated with growth-factor reduced Matrigel (BD Biosciences) in chemically defined medium (CDM; DMEM/F12+Glutamax, N2, B27 w/o vitamin A, 0.1 mM nonessential amino acids, 0.05% BSA Fraction V, pen/strep, 20 ng/ml bFGF (all from Invitrogen), and 0.1 mM 2-mercaptoethanol (Sigma Aldrich)) and cultured as described (Yao et al., 2006). At day 1, bFGF was removed and 100 ng/ml activin A and/or 25 ng/ml BMP4 (R&D systems) was added to the medium.

Transient overexpression

The cDNA of EVX1 and GSC was cloned into pENTR-TOPO/D vectors by directional PCR cloning followed by L/R recombination into pCGIG (Rosenberg et al., 2010). Expression vectors were transfected into hESC seeded at a density of 25000 cells/cm^2 using Fugene HD (Promega) according to manufacturer's instructions.

Generation of stable knockdown and overexpression cell lines

We used pTP6-hrGFP to generate GFP expressing control hESC (Pratt et al., 2000). After excision of hrGFP, *EVX1* and *T* cDNA was cloned into pTP6 to generate pTP6-EVX1 and pTP6-T. These vectors were Fugene HD transfected into hESC, seeded at a density of 25,000 cells/cm^2 in feeder-free conditions in CDM. Selection with 1 μg/ml puromycin was maintained for 10–14 days with daily medium changes. Stable knockdown ESC lines were generated using lentiviral particles harboring shRNA expression vectors targeting human EVX1 and T (Santa Cruz Biotechnology (SCBT)). MISSION® shRNA Lentiviral Transduction Particles targeting *GSC* as well as non-target specific control particles were purchased from Sigma. Seeding hESC was done in feeder-free conditions in CDM at a density of 25,000 cells/cm^2. ES cells were transduced with an MOI of 10 and selection with 1 μg/ml puromycin was started at day 2 and maintained for 8 days. Knockdown efficiency was assayed using qPCR and western blotting. Hairpin sequences are available upon request.

Flow cytometry

Cells were dissociated in 0.05% Trypsin-EDTA (Invitrogen) and resuspended in 1 mM EDTA (Invitrogen), 25 mM HEPES (Invitrogen), 1% BSA (Sigma Aldrich) in PBS. Sorting of GFP$^+$ and GFP$^-$ cells for RNA extraction was performed on a FACSAria (BD Biosciences).

Quantitative real-time RT-PCR

Extraction of total RNA was done with Nucleospin RNA II (Macherey-Nagel). Genomic DNA was removed by DNase I (Promega) treatment. cDNA was prepared from 250 to 500 ng RNA using iScript cDNA synthesis kit (Biorad). QPCR was performed using the standard SYBR® Green program with dissociation curve of the Mx3005P (Stratagene) and the Brilliant® SYBR® Green qPCR Master Mix (Stratagene). Quantified values for each gene of interest were normalized against the input determined by the housekeeping genes *G6pdh* and *TBP*. Primer sequences are available upon request.

Immunocytochemistry

Cells were fixed and stained as described (Hansson et al., 2009) using goat anti-Sox17, 1:1000 (R&D Systems). Cells were incubated with Cy3-conjugated species-specific secondary antibodies, 1:500 (Jackson ImmunoResearch Laboratories) and counterstaining of nuclei was performed with 4′,6-diamidino-2-phenylindole (DAPI, MP Biomedicals). Mounting was performed with mounting medium (KPL). Immunostaining was acquired using an LSM 510 META laser scanning microscope (Carl Zeiss) and the Axiovision software (Carl Zeiss, Inc.) or Olympus IX81 inverted microscope (Olympus) with camera (Olympus DP71) and the CellP software (Olympus). For quantification, 9 images per well of each condition were captured randomly using a motorized stage on the Olympus IX81 inverted microscope with Olympus DP71 camera and CellP software (Olympus). Quantification was performed using automated image analysis software, Cellc (Selinummi et al., 2005).

Western blotting

Total cell lysates were made in lysis buffer (Cell Signaling Technologies). 20 μg of each sample was loaded and separated on 10% Bis-tris polyacrylamide gels (NuPage, Invitrogen), transferred onto PVDF membranes (Invitrogen) and detected through HRP-conjugated antibodies (Santa Cruz Biotechnology) and chemiluminisence (ECL plus, Amersham). Primary antibodies used were: goat anti-Sox17, 1:1000 (R&D systems); goat anti-Brachyury, 1:1000 (R&D systems); goat anti-GSC, 1:500 (Santa Cruz Biotechnologies); rabbit anti-EVX1, 1:500 (human, Sigma-Aldrich); mouse anti-ß-Actin, 1:25000 (Sigma-Aldrich); rabbit anti-TFIIbeta, 1:2000 (Santa Cruz Biotechnologies).

ChIP analysis

Human ES cells were differentiated for 1 day with 25 ng/ml BMP4 and ChIP was performed with the ChampionChIP™ One-Day Kit (SABiosciences). Sonication (16 pulses of 30 seconds bursts with an amplitude of 32% on a Branson sonicator) yielded fragment sizes of 1–3 kb. Samples were immunoprecipitated with 4 μg rabbit anti-human EVX1 (Sigma-Aldrich), 4 μg mouse anti-human RNA polymerase II for the positive control (SABiosciences) or the corresponding isotype controls: rabbit IgG (for EVX1) or mouse IgG2A (for human polII). After crosslink reversal and DNA isolation, fractions were analyzed by qPCR. Primers amplifying 100–200 bp products were placed for every ~800 bp of the 5′-region from transcription start site to −10 kb. Primer sequences are listed in Table S1.

Electrophoretic mobility shift assay (EMSA)

Nuclear extracts (NE) were prepared from H9 hESC cultures treated for 1 day with either control (BSA) or BMP4. Binding reactions contained 5 μg of NE, incubated for 20 minutes at 25 °C with α^{32}P-dCTP labeled double-stranded oligos containing putative binding sequences of EVX1 in a reaction buffer containing 10% glycerol, 25 mM HEPES, 1 mM EDTA, 50 mM NaCl, 0.5 mM DTT as well as

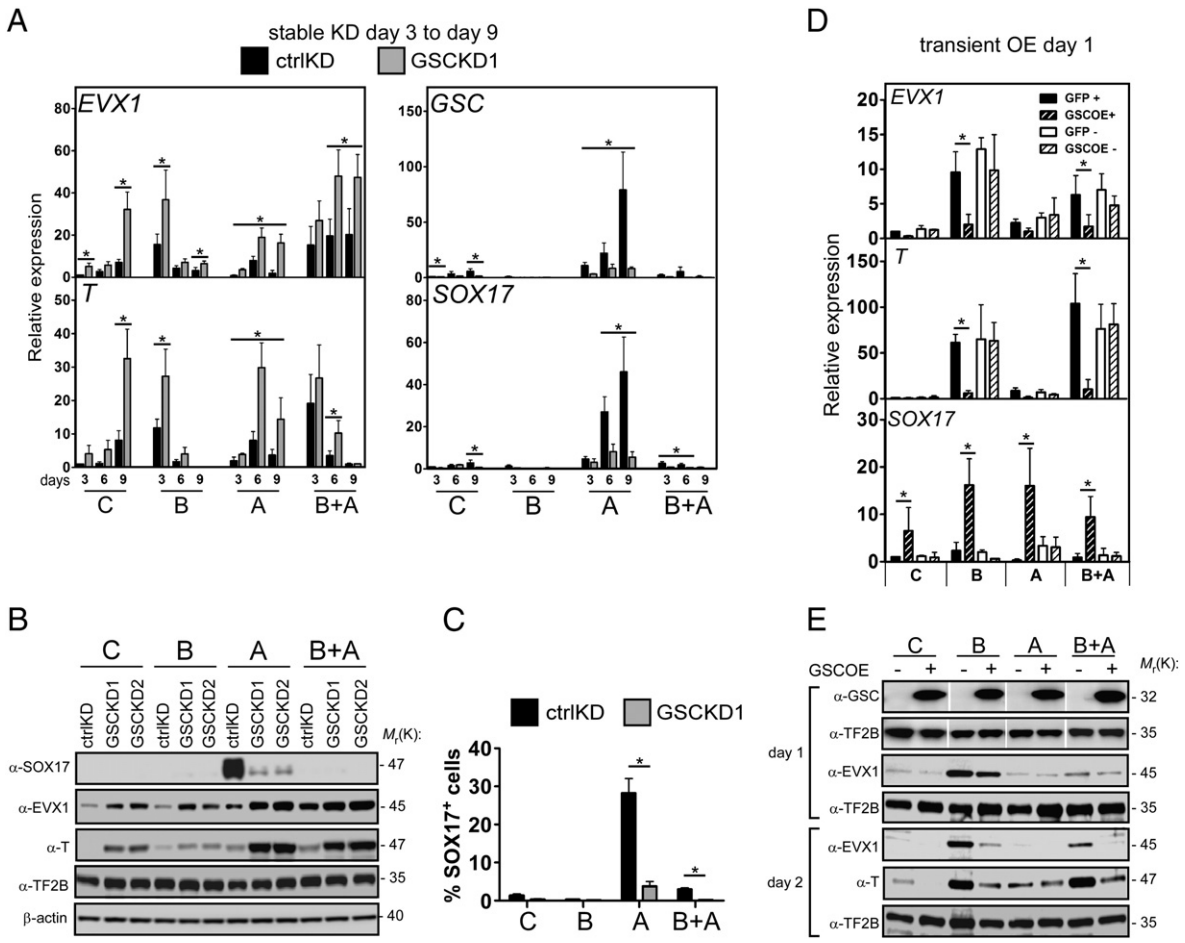

Fig. 1. GOOSECOID inhibits posterior streak and mesodermal cell fates and is required for development of anterior streak descendants in hESC. (A) Stable knockdown H9 hESC lines expressing a non-target specific control shRNA (ctrlKD) or a GSC targeting shRNA (GSCKD1) were differentiated for 3, 6 and 9 days and harvested for qPCR. Cells were treated with BSA (C), BMP4 (B), activin A (A) or BMP4+activin A (B+A) for 3-9 days. (B) Protein levels of SOX17, EVX1 and in ctrlKD, GSCKD1 and GSCKD2 hESC lines at day 6 of differentiation. TF2B and ß-actin was used as loading control. (C) Quantification of immunostaining of SOX17 in differentiated ctrlKD-hESC and GSCKD1-hESC at day 6 of differentiation. SOX17 positive cells were quantified as percentage of total cells (DAPI staining of nuclei). (D) Gene expression analysis of FACS sorted hESC transiently overexpressing GFP or GSC-IRES-GFP. Cells were transfected and treated with BSA (C), BMP4 (B), activin A (A) or BMP4+activin A (B+A) for 1 day. The overexpressing (GFP+ and GSCOE+) and non-expressing (GFP- and GSCOE-) populations were sorted and processed for qPCR. (E) Levels of GSC, EVX1 and T protein in H9 hESC transiently overexpressing GFP (−) or GSC-IRES-GFP (GSCOE) (+) harvested at day 1 or 2 of differentiation. Notice the stronger decrease of EVX1 at day 2. TF2B was used as loading control. Data represent the mean of $n=3$ normalized to the untreated (C) condition in the ctrlKD cell lines. Error bars indicate SEM. $^{*}p<0.05$ compared to ctrlKD cell lines.

2 μg poly-dIdC and 2 μg poly-dGdC. Competition analysis was performed with 25- and 50-fold molar excess of unlabeled wild-type or mutant oligos. For supershift assays, 250 ng of anti-Evx1 antibody (DSHB) was added to the binding reaction and isotype matched IgG was used as control. Reaction products were separated on a 6% non-denaturing polyacrylamide gel in 0.5× Tris-borate-EDTA at 10 V/cm for 1 hour at room temperature and visualized on a phosphoimager. The sequences of the probes were: BS1: 5′-GATCCTTGCTAATCATTTCA-3′; BS2: 5′-GATCCCTTTTAATCCCAAAA-3′; BS3.; 5′-GATCCACTGATTAGCTCGGA-3′. Mutant binding site oligonucleotides contained AA to CC substitutions in the "TAAT" core homeodomain binding sequence.

Generation of reporter constructs and luciferase assays

6.2 kb of the *GSC* 5′-region was PCR cloned from hESC genomic DNA and inserted into *SacI*/*XhoI* sites of the pTA-luc vector (Clonetech) to generate the pTA-*GSC*-luc reporter. PCR products covering the −5.1 kb to −4.0 kb region of the *GSC* gene were inserted into *MluI*/*XhoI* sites in a pSV40-TA-luc vector. Constructs containing mutant EVX1 binding sites were generated by site-directed mutagenesis of the core homedomain binding motifs (AA to CC) as shown in Fig. 3G. The pTA-*GSC*-luc reporters were co-transfected with pCMV-renilla into H9 hESC treated with 25 ng/ml BMP4, 100 ng/ml activin A or BMP4+activin A. Heterologous promoter constructs were co-transfected with pCMV-renilla and pTP6-EVX1 into HEK-293T cells. The amount of expression vector was kept constant by addition of pTP6-hrGFP. Cells were harvested after 24 hours and luciferase and renilla activities were assayed. The relative promoter activities were expressed as the fold-change after normalization to renilla activity.

Statistics

Mean relative expression (qPCR) ± standard error of the mean (SEM) was calculated. Asterisks indicate significantly changes from control groups ($p<0.05$) by a two-tailed Student's *t*-test or two-way ANOVA with Bonferroni correction for multiple comparisons.

Results

Activin and BMP4 induce anterior and posterior genes, respectively, in human ES cells

Nodal/activin dose-dependently drives differentiation of mouse and human ES cells through streak-like progenitor stages towards anterior mesoderm and definitive endoderm (DE) (D'Amour et al.,

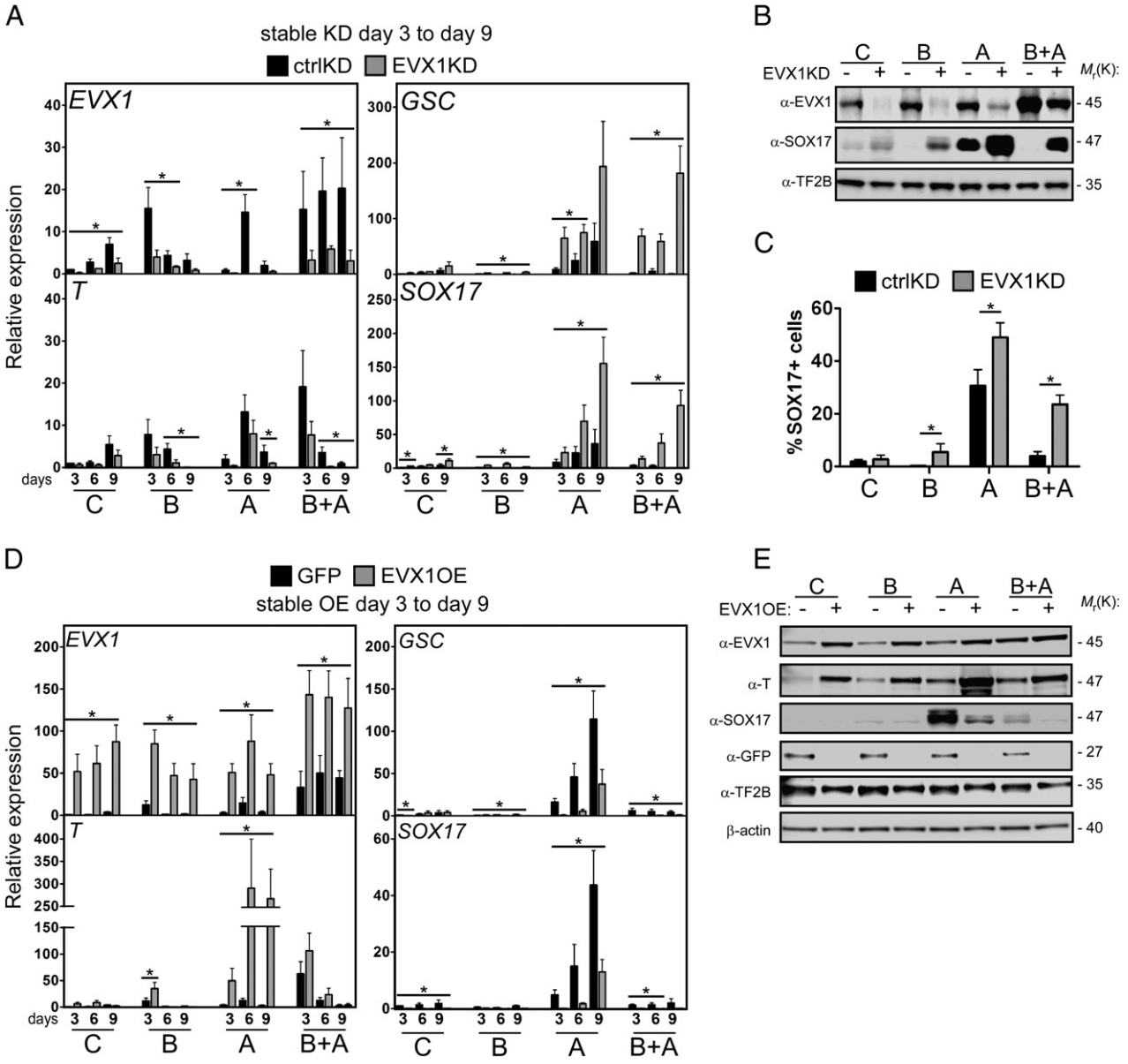

Fig. 2. EVX1 inhibits anterior streak and DE formation and induces posterior streak/mesoderm differentiation in hESC. (A) Analysis of gene expression in EVX1KD-hESC and ctrlKD-hESC lines. (B) Protein levels of EVX1 and SOX17 in stable knockdown hESC lines expressing a non-target control shRNA, ctrlKD (−) or an EVX1 targeting shRNA, EVX1KD (+) at day 6 of differentiation. TF2B was used as loading control. (C) Quantification of SOX17 immunostaining in differentiated ctrlKD-hESC and EVX1KD-hESC at day 6 of differentiation. SOX17 positive cells were quantified as percentage of total cells (DAPI staining of nuclei). (D) Gene expression levels in stable GFP or EVX1 overexpression hESC lines (GFP or EVX1OE, respectively) analyzed after 3, 6 and 9 days of differentiation. (E) Protein levels of EVX1, T, SOX17 and GFP at day 6 of differentiation in stable GFP (−) or EVX1 (+) overexpression hESC lines. TF2B and ß-actin was used as loading control. Cells were treated with growth factors as in Fig. 1. Data represent the mean of $n=3$ normalized to the untreated (C) condition in the ctrlKD cell lines. Error bars indicate SEM. $^{*}p<0.05$ compared to ctrlKD cell lines.

2005; Hansson et al., 2009; Kubo et al., 2004; Tada et al., 2005), while BMP4 induces posterior streak-like and mesodermal fates (Hansson et al., 2009; Nostro et al., 2008; Zhang et al., 2008) and in hESC also extraembryonic cell types (Xu et al., 2002). To gain further insight into the mechanisms that govern cell fate decisions in response to TGFß signals we first characterized BMP4- and activin-induced gene expression pattern in hESC. Treatment of hESC with BMP4 alone resulted in a rapid and transient induction of the posterior streak/mesoderm markers *EVX1*, *T* and *BAMBI* (Alev et al., 2010; Bastian and Gruss, 1990; Dush and Martin, 1992; Grotewold et al., 2001; Onichtchouk et al., 1999; Wilkinson et al., 1990), and a later induction of the mesoderm marker *TWIST1* (Fig. S1A and S1B and Table S2); (Fuchtbauer, 1995; Wolf et al., 1991). Conversely, treatment with activin alone induced expression of *GSC*, *SOX17*, *LIM1*, and *CXCR4* (Fig. S1 and Table S2), markers of anterior streak and DE (Ang et al., 1993; Barnes et al., 1994; Kanai-Azuma et al., 2002; McGrath et al., 1999; Yasunaga et al., 2005). As observed previously in other systems (Hansson et al., 2009; Jones et al., 1996; Nostro et al., 2008), the posteriorizing activity of BMP4 was dominant over the anteriorizing activity of activin when both growth factors were added. Anterior streak/DE markers were suppressed over the entire differentiation period whereas expression of posterior streak/mesoderm markers was prolonged (Fig. S1 and Table S2). As expected (Pera et al., 2004; Wu et al., 2008; Xu et al., 2002), markers of extraembryonic tissues like visceral endoderm (*SOX7*, (Kanai-Azuma et al., 2002)) and trophectoderm (*hCGß*, (Muyan and Boime, 1997)) were induced by BMP4 but completely suppressed

by added activin (Table S2). Expression of the neuroectoderm marker *SOX1* (Pevny et al., 1998) was suppressed by either BMP4 or activin as previously reported (Schuldiner et al., 2000; Ying et al., 2003) and *OCT4* was decreasing over the differentiation period (Table S2). Similar results were obtained in two hESC lines (H9 and SHEF3 (Fig. S1 and data not shown).

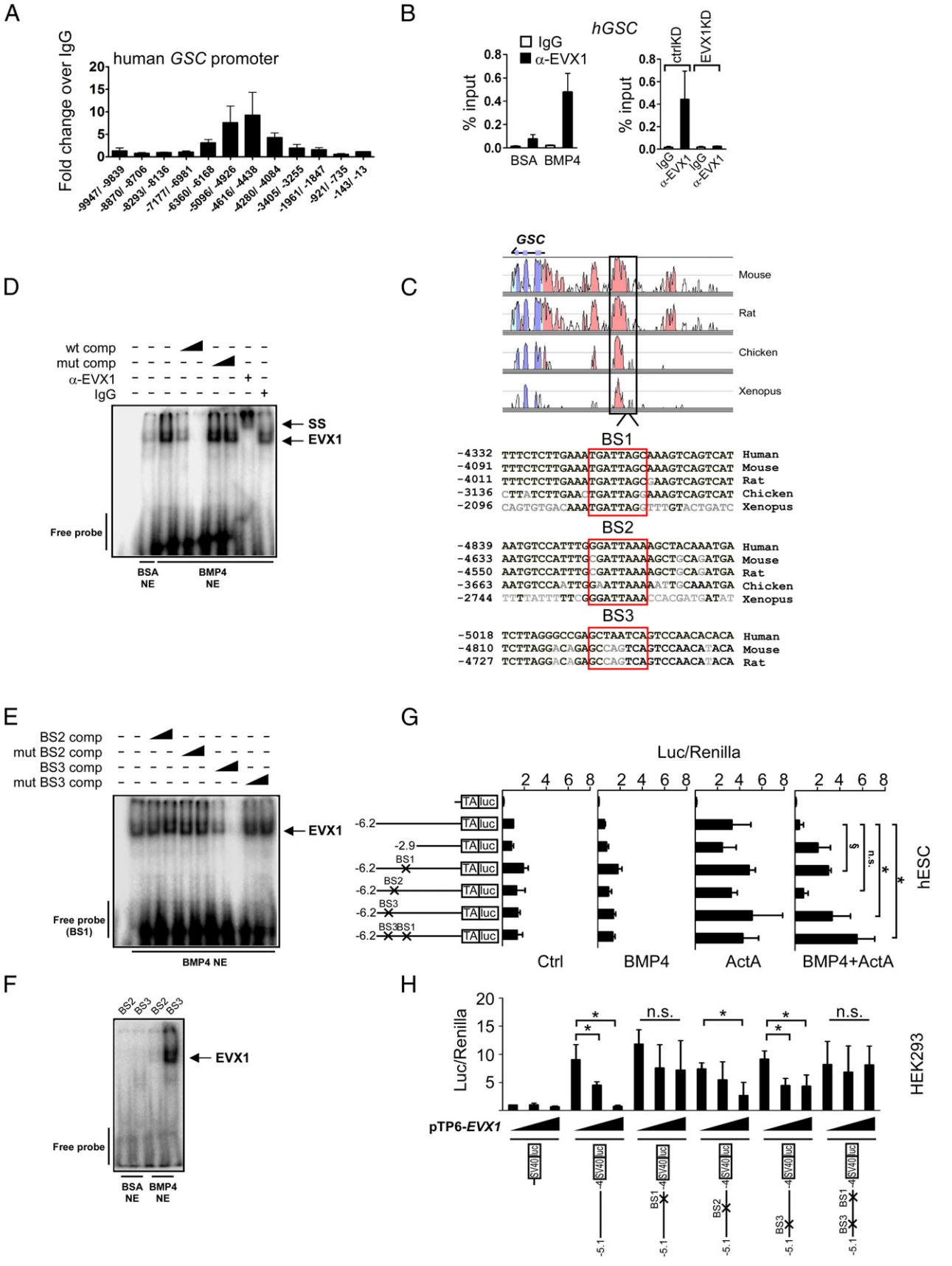

GSC anteriorizes streak-like ES cell progeny and is required for anterior streak/definitive endoderm formation in human ES cells

To begin to understand the role of *GSC* and *EVX1* in activin- and BMP-induced A–P patterning of streak-like ES cell descendents we first investigated the function of *GSC* by shRNA mediated knockdown. Knockdown of GSC did not affect pluripotency as judged by expression of pluripotency markers in undifferentiated GSCKD-hESC lines (data not shown). Initial short term experiments in hESC showed that knockdown of *GSC* increased *EVX1* and *T* transcripts as well as their cognate proteins (data not shown). To analyze the effects of *GSC* depletion at later stages of differentiation we generated stable *GSC* knockdown hESC (GSCKD-hESC) lines and analyzed differentiation by qPCR and immunocytochemistry (ICC) after activin and/or BMP4 treatment. QPCR analysis showed an increase of *EVX1* and *T* transcripts in H9 GSCKD-hESC lines compared to control knockdown hESC (ctrlKD-hESC) lines, whereas *SOX17* was suppressed (Fig. 1A). Western blots confirmed that the increase of EVX1 and T protein was accompanied by reduced activin-induced SOX17 expression after *GSC* knockdown (Fig. 1B). Quantitative ICC revealed a ~10-fold reduction of $SOX17^+$ cells on day 6 in activin treated H9 GSCKD-hESC compared to control cell lines (Fig. 1C). The qPCR, western blots and quantitative ICC data were confirmed in hESC expressing a different *GSC*-targeting shRNA sequence and identical results were obtained by knocking down *GSC* in H9 and SHEF3 hESC (Fig. 1A–C and data not shown).

To further examine the role of *GSC* we next overexpressed *GSC* transiently in H9 hESC, isolated the overexpressing and non-expressing populations by FACS sorting, and monitored differentiation after activin and/or BMP4 treatment. Consistent with the knock down results, qPCR analyses showed that *EVX1* and *T* were repressed in the *GSC* overexpressing population 1 day after growth factor provision suggesting, a cell-autonomous repression of these genes (Fig. 1D). This repression was confirmed at the protein level which also revealed a more pronounced decrease of both markers on day 2 (Fig. 1E). Conversely, *SOX17* transcript was increased when *GSC* was overexpressed (Fig. 1D). Similar results were obtained in non-sorted SHEF3 hESC overexpressing *GSC* (Fig. S2A). Attempts to generate stable *GSC* overexpressing hESC lines failed, possibly due to adverse effects of *GSC* overexpression on cell viability or hESC pluripotency.

Loss of EVX1 anteriorizes streak-like hESC progeny and reverses BMP4 induced suppression of DE formation

The above results suggest that GSC inhibits posterior development via repression of EVX1. To determine if EVX1 was required for efficient development of posterior streak-like cells, we carried out loss-of-function experiments, knocking down EVX1 in hESC with shRNA and generated target-specific knockdown and control knockdown cell lines (EVX1KD-ESC and ctrlKD-ESC, respectively). EVX1KD-ESC lines were indistinguishable from wild-type ESC in terms of morphology and pluripotency marker expression prior to differentiation experiments (data not shown). Analysis of knock down efficiency by qPCR showed that *EVX1* mRNA was reduced by >60% in all conditions and time points in EVX1KD-hESC compared to ctrlKD-hESC (Fig. 2A) which was confirmed at the protein level on day 6 of differentiation (Fig. 2B). When analyzing A–P marker expression we found that *T* was significantly reduced in EVX1KD-hESC while activin-induced *GSC* and *SOX17* expression was strongly increased compared to ctrlKD-hESC (Fig. 2A). Notably, BMP4 could no longer suppress activin-induced anterior streak/DE markers (Fig. 2A and B). As a result, the number of activin-induced $SOX17^+$ cells was increased from 30.6% ± 6.1% in the ctrlKD-hESC line to 49.0% ± 5.5% in EVX1KD-hESC at day 6 (Fig. 2C). BMP4 was also less effective in preventing activin-mediated induction of $SOX17^+$ cells in EVX1KD-hESC (~2-fold reduction) compared to ctrlKD-hESC (~8-fold reduction; Fig. 2C). Similar results were obtained in SHEF3 EVX1KD-hESC (data not shown).

EVX1 posteriorizes streak-like ESC progeny

To further explore the function of EVX1 during ES cell differentiation, we then overexpressed *EVX1* in hESC. H9 hESC were transiently transfected with an *EVX1*expression plasmid, treated with BMP4 and/or activin for 24 hours, and the overexpressing and non-expressing populations were isolated by FACS sorting and processed for qPCR. Transient *EVX1* overexpression was found to reduce activin-induced *GSC* expression and increase *T* expression specifically in the expressing population, suggesting a cell-autonomous effect. This effect was observed under all growth factor conditions and confirmed in SHEF3 hESC (Fig. S2B and S2C). To test if EVX1 could suppress anterior markers at later stages where their expression normally peak we generated stable hESC lines overexpressing *EVX1* or GFP as control (EVX1OE-hESC and GFP-hESC, respectively). Overexpression of *EVX1* (or GFP) did not affect expression of pluripotency markers in undifferentiated hESC (data not shown). We cultured EVX1OE-hESC and GFP-hESC in BMP4 and/or activin before assaying expression of A–P markers by qPCR and western blotting and found that Activin-, and to a lesser extent also BMP4-induced *T* expression was elevated in EVX1OE-hESC (Fig. 2D). In contrast, activin-induced *GSC* and *SOX17* expression was markedly reduced (Fig. 2D). The same pattern of regulation of T and SOX17 was observed at the protein level (Fig. 2E). Taken together, these results suggest that EVX1 represses anterior streak/DE markers in hESC while enhancing differentiation of posterior streak cells and mesoderm.

EVX1 binding to the GSC promoter is required for BMP4-induced repression

The above results suggest that EVX1 represses *GSC* expression in BMP4 treated, streak-like human ES cell progeny. Because previous studies have shown that EVX1 can act as a repressor (Briata et al., 1995, 1997), we used ChIP analysis to determine if EVX1 bound to the *GSC* promoter in BMP4 treated ES cells. We detected binding of EVX1 to a conserved region of the *GSC* promoter located ~4.0

Fig. 3. EVX1 binds to a conserved region of the *GSC* promoter. (A) H9 hESC were treated with BMP4 for 1 day and binding of EVX1 to the *GSC* 5′-region was analyzed by ChIP followed by qPCR using primers spanning the denoted regions for detection of enrichment as shown by the mean fold change over IgG of three independent experiments. (B) ChIP analysis of the *GSC* 5′-region in wild-type H9 hESC treated for 1 day with BSA or BMP4 (left panel) and in ctrlKD or EVX1KD hESC cultures treated with BMP4 for 1 day (right panel) using primers spanning the region with highest enrichment in Fig. 3A. Enrichment is plotted as percentage of 2% input DNA and IgG served as a control. Error bars represent SD of three independent experiments. (C) Vista Genome alignment of different vertebrate species of the *GSC* promoter region against the human *GSC* promoter sequence. Highly conserved regions are illustrated as peaks (pink). EVX1 binding is located in a conserved region about 4.3–5 kb upstream of the *GSC* transcriptional start site. Within this region a binding site of the EVX1 homologue even-skipped (*Drosophila*) was present (BS1) and two other putative sites (BS2 and BS3), all containing the core EVX1 homeodomain binding sequence, GATTA. (D) EMSA using nuclear extracts (NE) from H9 hESC untreated (BSA) or treated with 25 ng/ml BMP4 for 1 day. EVX1 complexes are indicated by the arrow as well as the supershifted complex (SS). Competition assay was performed by adding unlabeled wild-type or mutant BS1 probes (wt comp and mut comp, respectively) at 25-fold or 50-fold molar excess. (E) EMSA competition assay. NE from 1 day BMP4 treated H9 hESC were incubated with labeled BS1 probe and competition was performed with unlabeled wild-type or mutant probes for BS2 and BS3 at 25-fold or 50-fold molar excess. (F) EMSA performed with NE from untreated or BMP4 treated H9 hESC incubated with labeled BS2 or BS3 probes. EVX1 complexes are indicated by the arrow. (G) Luciferase assays using *GSC* reporter constructs (wild-type −6.2 kb, truncated −2.9 kb as well as BS1, BS2, BS3, and BS1BS3 mutations of the *GSC* 5' region) were transiently transfected into H9 hESC and subsequently treated with the indicated growth factors for 24 hours. Error bars indicate SD. $^*p<0.05$, §$p<0.005$. n.s. = not significant. $n=3$ compared to the wild-type construct. (H) Luciferase assays showing that the −4.0 to −5.1 kb fragment of the *GSC* 5′ region confers EVX1-dependent repression on the SV40 enhancer in HEK 293 cells. Error bars indicate SD. $^*p<0.05$, $n=3$.

to ~6.4 kb upstream of the *GSC* transcription start site (Fig. 3A). The ChIP signal was detected in chromatin from BMP4 treated hESC progeny, but not in chromatin from spontaneously differentiating, BSA treated hESC progeny or chromatin from BMP4-treated EVX1KD hESC (Fig. 3B) confirming the specificity of the EVX1 antibody. Within the area of the *GSC* 5′-region are numerous potential binding sites for homeodomain proteins, including three occurrences of the core sequence GATTA (Fig. 3C) present in known Evx1 binding sites (Hoey and Levine, 1988; Maulbecker and Gruss, 1993). To test if any of these putative EVX1 binding sites were functional we first used EMSA to define the sequences capable of binding EVX1. We found that two out of the three putative binding sites (BS1 and BS3) were capable of binding a factor specifically present in nuclear extracts from BMP4 stimulated hESC progeny (Fig. 3D–F). Competition experiments demonstrated that binding was sequence specific and dependent on an intact TAAT core motif. Moreover, pre-incubation with a monoclonal anti-EVX1 antibody was capable of supershifting the complex (Fig. 3D), and pre-incubation with a polyclonal anti-EVX1 antiserum prevented complex formation (data not shown).

To test if these two EVX1 binding sites were required for BMP4-mediated repression of *GSC*, we generated wild-type and mutant luciferase reporter constructs encompassing the relevant region of the *GSC* 5'-region and transfected these into hESC and stimulated with BMP4 and/or activin A. We found that BMP4 was capable of repressing activin-induced activity from a −6.2 kb *GSC* reporter including the EVX1 binding sites, but was unable to repress activity of a truncated −2.9 kb *GSC* reporter lacking the EVX1 binding sites. Moreover, mutating either BS1 or BS3 in the −6.2 *GSC* reporter reduced the ability of BMP4 to repress luciferase activity while mutating both sites eliminated BMP4-induced repression of reporter activity (Fig. 3G). Additionally, a −5.1 to −4.0 kb fragment of the *GSC* promoter, containing BS1 and BS3, conferred dose-dependent repression by EVX1 when placed in front of a SV40-enhancer driven luciferase reporter. Crucially, mutating either BS1 or BS3 reduced the ability of EVX1 to repress luciferase activity while mutating both sites eliminated EVX1-mediated repression of reporter activity (Fig. 3H).

Conserved interactions between T, EVX1, and GSC in hESC

The results so far demonstrate that GSC and EVX1 occupy a central position in a GRN that governs mesendodermal cell fates downstream of TGFß signaling. Studies in mice, *Xenopus*, and Zebrafish have uncovered that T is a key regulator of posterior mesoderm development (Showell et al., 2004; Wardle and Papaioannou, 2008) and that *Xbra* (the *Xenopus* ortholog of T) is interacting with both *Xgsc* and *Xhox3* (Cunliffe and Smith, 1992; Gurdon and Bourillot, 2001; Latinkic et al., 1997). To determine if T occupies a similar place in the regulatory network operating in hESC we therefore performed gain- and loss-of-function analysis of T in hESC and analyzed their response to activin and/or BMP4 stimulation. We created stable hESC lines, with either elevated or reduced levels of T (TOE-hESC and TKD-hESC, respectively). TOE-hESC expressed 30- to 50-fold higher *T* levels than GFP-hESC in the control condition, a level corresponding to endogenous *T* expression on day 3 in GFP-hESC when treated with BMP4 and activin (Fig. 4A). We obtained approximately 70% knockdown efficiency of *T* which was maintained over the entire time-course of differentiation (Fig. 4B) and verified reduction of T protein by western blotting (Fig. 4C). Neither overexpression nor knockdown of T affected expression of pluripotency markers during maintenance of the cell lines (data not shown).

Expression of *EVX1* was induced when T was overexpressed and this induction was most prominent upon differentiation in the presence of activin (Fig. 4A). Conversely, knockdown of T, resulted in reduction of *EVX1* transcripts (Fig. 4B), demonstrating that T stimulates *EVX1* expression in hESC. In activin treated hESC, T stimulated *GSC* expression on day 3, showed no effect on day 6, and repressed *GSC* on day 9 (Fig. 4A). Similarly, T overexpression induced *SOX17* expression on day 3, possibly via its effect on GSC expression, followed by a progressive suppression on days 6 and 9, consistent with the strong induction of *EVX1* which would repress *GSC* expression at this stage (Fig. 4A). As predicted from the overexpression results, knockdown of T caused a reduction in *EVX1* expression but stimulated activin-induced *GSC* and *SOX17* expression strongly and prevented BMP4 from repressing these genes in the presence of activin and BMP4 (Fig. 4B). Western blotting confirmed upregulation of SOX17 protein levels (Fig. 4D) and ICC revealed that almost 70% of the cells became $SOX17^+$ on day 6 when TKD-hESC were treated with activin and BMP4, a 17-fold increase compared to ctrlKD hESC (Fig. 4E).

Discussion

Here we show that mutually inhibitory interactions between *GSC* and *EVX1* form the core of a GRN which mediate anterior–posterior patterning of streak-like hESC descendents in response to nodal/activin and BMP signaling. Our results extend previous in vivo studies showing that mutual repression between *GSC* and *EVX1* homologs plays a key role in the A–P patterning of gastrulating cells in fish and amphibian (Cho et al., 1991; Imai et al., 2001; Kawahara et al., 2000; Melby et al., 2000; Niehrs et al., 1993, 1994; Ruiz i Altaba and Melton, 1989a,b; Ruiz i Altaba et al., 1991; Sander et al., 2007; Steinbeisser et al., 1995), and suggests that the function of this GRN is conserved in mammalian streak patterning in spite of the lack of gastrulation defects in *Gsc* and *Evx1* deficient mouse embryos (Moran-Rivard et al., 2001; Rivera-Perez et al., 1995; Yamada et al., 1995).

The promotion of anterior streak- and DE-like fates in hESC overexpressing *GSC* is comparable to the strong dorsalizing effect seen after injection of *Xgsc* mRNA into the ventral half of *Xenopus* embryos (Cho et al., 1991; Niehrs et al., 1993, 1994). The loss of anterior, and gain of posterior markers observed after *GSC* knockdown is consistent with our gain-of-function data and with the ventralized phenotype of *Xenopus* embryos resulting from *Xgsc* knockdown (Sander et al., 2007; Steinbeisser et al., 1995). Notably, when *EVX1* was overexpressed in hESC we saw a reduction of *GSC* transcripts and a corresponding induction of *T* expression. These changes resemble defects in the A–P patterning of axial mesoderm, including loss of anterior structures seen in *Xhox3* overexpressing *Xenopus* embryos (Ruiz i Altaba and Melton, 1989b). A function of *EVX1* in posterior streak development is supported by our loss-of-function experiments which caused reduced expression of *T* in EVX1KD-hESC and promotion of anterior streak fates and DE formation. Similar effects are observed after Xhox3 antibody blocking experiments in *Xenopus* which results in posterior defects (Ruiz i Altaba et al., 1991). Our studies indicate that EVX1 is an important regulator of streak development in hESC and suggest that EVX1 alone is sufficient to carry out the function of the Vent1/2-Xhox3 "cassette". This notion is supported by our identification of two EVX1 binding sites in the *GSC* 5′-region that are required for BMP4-induced repression of *GSC*.

Increased formation of endoderm after EVX1/Xhox3 inhibition has to our knowledge not been reported previously and offers a route to more efficient formation of therapeutically relevant cell types. By attenuating expression of transcription factors or "deprogramming" hESC one can increase the number of desired cell types by avoiding differentiation in unwanted directions as demonstrated in this study for endoderm formation.

In *Xenopus*, repression of *Xgsc* by BMP signaling has been suggested to rely on induction of *Xbra* (*T*) followed by Xbra induction of Vent1/2, which subsequently repress *Xgsc* expression (Messenger et al., 2005). In addition, Xbra mediated suppression of *Xgsc* through Vent1/2 was shown to be dependent on direct interaction of Xbra with Smad1 which required BMP signaling (Messenger et al., 2005). By compromising this interaction or if Vent1/2 was depleted, *Xgsc* was prominently induced by Xbra. We show here that *GSC* is

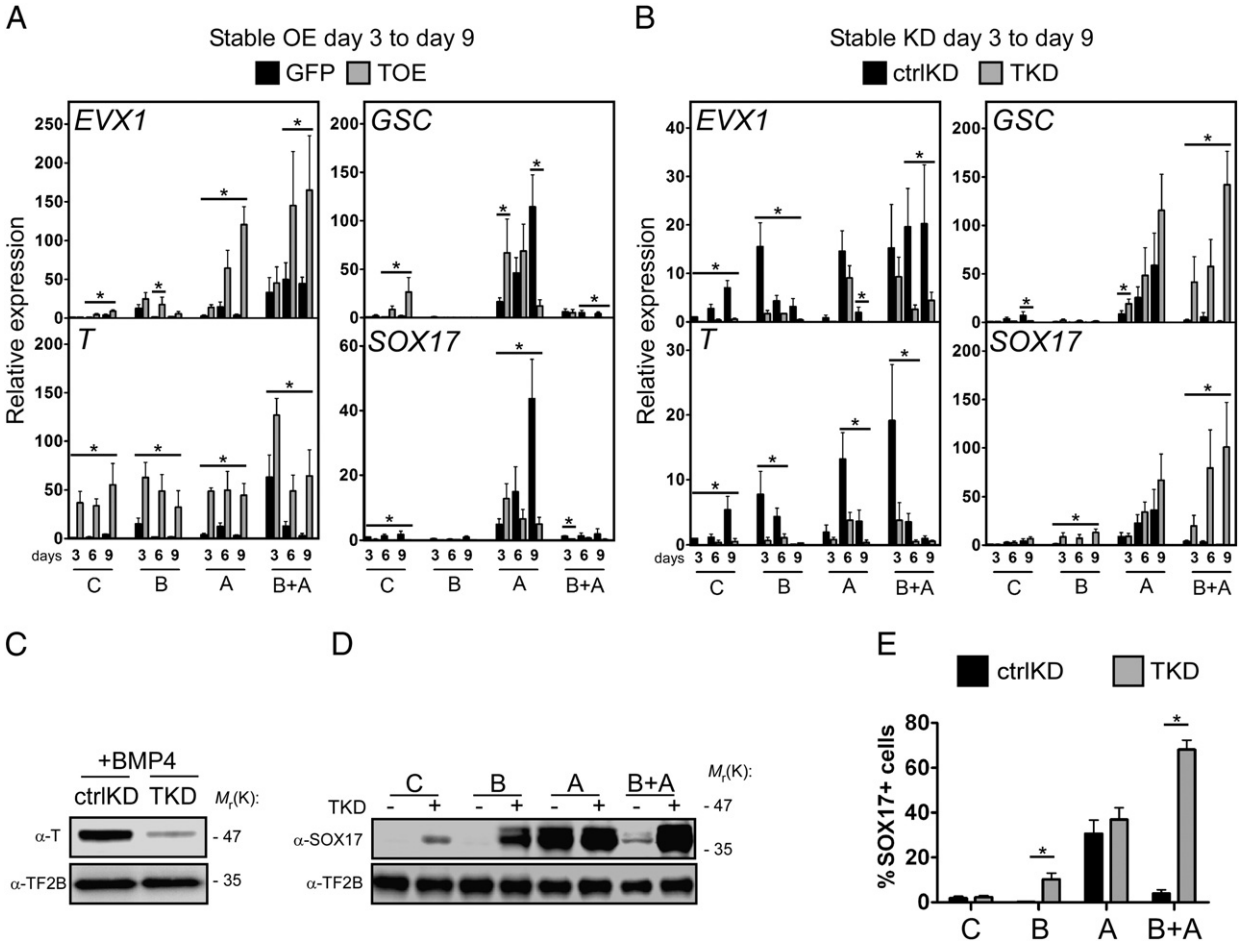

Fig. 4. T interacts with EVX1 and GSC in hESC. (A) Expression analysis of posterior and anterior streak genes in stable hESC overexpression cell lines expressing either GFP or T. (B) Gene expression analysis in stable hESC knockdown cell lines expressing a non-target specific control shRNA (ctrlKD) or a T targeting shRNA (TKD). (C) Western blots showing T knockdown at the protein level. TF2B was used as loading control. (D) Western blots showing SOX17 protein levels in ctrlKD (−) and TKD (+) hESC lines at day 6 of differentiation. TF2B was used as loading control. (E) Quantification of SOX17 immunostaining relative to nuclear DAPI stain in differentiated ctrlKD- or TKD-hESC at day 6 of differentiation. Data represent the mean of three independent experiments normalized to the untreated (C) condition in the GFP expressing control (overexpression) or ctrlKD (knock-down) cell lines. Error bars indicate SEM. $^*p<0.05$ compared to GFP or ctrlKD cell lines.

repressed by BMP4 dependent on *EVX1*. Since T is a transcriptional activator (Conlon et al., 1996; Kispert and Hermann, 1993; Kispert et al., 1995) we hypothesize that T induce or maintain *EVX1* expression resulting in the observed *GSC* repression. The decreased *EVX1* expression and increased *GSC* expression following knockdown of T seen in our study is consistent with a requirement for *T* in the maintenance of *Evx1* expression in mice (Rashbass et al., 1994). Taken together our results show that GSC and EVX1 interact with each other as well as with T in a GRN (Fig. 5) that mediate cell fate choices in response to TGFβ family signaling during streak-like development of hESC, and that EVX1 acts through direct repression of *GSC*.

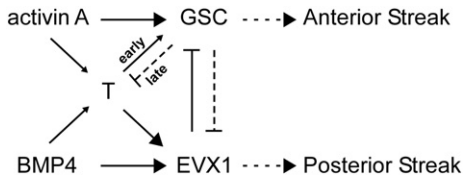

Fig. 5. GSC, EVX1 and T occupy central positions in a gene regulatory network controlling mesendoderm cell fates. Opposing interactions between GSC and EVX1 regulate mesendodermal differentiation to anterior- or posterior-streak descendants. In the presence of activin, GSC and T are induced. When the levels of GSC protein build up during prolonged differentiation, T and EVX1 are inhibited by GSC thereby allowing differentiation to proceed toward anterior streak-fates such as endoderm. BMP4 induces T and EVX1 (possible through T). EVX1 in turn represses GSC resulting in posterior-streak progression.

Supplementary materials related to this article can be found online at doi:10.1016/j.ydbio.2011.11.017.

Acknowledgements

We thank Drs. Ludovic Vallier and Claudia M. Palena for plasmids, Kristine Williams and Agnete Kirkeby for technical advice, and Tove Daa Funder-Nielsen, Ragna Jørgensen, Søren Refsgaard Lindskog, Heidi Ingemann Jensen, and Helene Brostrøm for technical assistance.

This work was supported by EU 6th Framework Program, the Juvenile Diabetes Research Foundation (grant # 1-2007-1048 and 35-2008-626), and the Danish Stem Cell Doctoral School (DASCDOC).

None of the authors have any competing financial interests.

References

Alev, C., Wu, Y., Kasukawa, T., Jakt, L.M., Ueda, H.R., Sheng, G., 2010. Transcriptomic landscape of the primitive streak. Development 137, 2863–2874.

Ang, S.L., Wierda, A., Wong, D., Stevens, K.A., Cascio, S., Rossant, J., Zaret, K.S., 1993. The formation and maintenance of the definitive endoderm lineage in the mouse: involvement of HNF3/forkhead proteins. Development 119, 1301–1315.

Bachiller, D., Klingensmith, J., Kemp, C., Belo, J.A., Anderson, R.M., May, S.R., McMahon, J.A., McMahon, A.P., Harland, R.M., Rossant, J., De Robertis, E.M., 2000. The organizer factors Chordin and Noggin are required for mouse forebrain development. Nature 403, 658–661.

Barnes, J.D., Crosby, J.L., Jones, C.M., Wright, C.V., Hogan, B.L., 1994. Embryonic expression of Lim-1, the mouse homolog of Xenopus Xlim-1, suggests a role in lateral mesoderm differentiation and neurogenesis. Dev. Biol. 161, 168–178.
Bastian, H., Gruss, P., 1990. A murine even-skipped homologue, Evx 1, is expressed during early embryogenesis and neurogenesis in a biphasic manner. EMBO J. 9, 1839–1852.
Briata, P., Ilengo, C., Van DeWerken, R., Corte, G., 1997. Mapping of a potent transcriptional repression region of the human homeodomain protein EVX1. FEBS Lett. 402, 131–135.
Briata, P., Van De Werken, R., Airoldi, I., Ilengo, C., Di Blas, E., Boncinelli, E., Corte, G., 1995. Transcriptional repression by the human homeobox protein EVX1 in transfected mammalian cells. J. Biol. Chem. 270, 27695–27701.
Cho, K.W., Blumberg, B., Steinbeisser, H., De Robertis, E.M., 1991. Molecular nature of Spemann's organizer: the role of the Xenopus homeobox gene goosecoid. Cell 67, 1111–1120.
Conlon, F.L., Sedgwick, S.G., Weston, K.M., Smith, J.C., 1996. Inhibition of Xbra transcription activation causes defects in mesodermal patterning and reveals autoregulation of Xbra in dorsal mesoderm. Development 122, 2427–2435.
Cunliffe, V., Smith, J.C., 1992. Ectopic mesoderm formation in *Xenopus* embryos caused by widespread expression of a Brachyury homologue. Nature 358, 427–430.
D'Amour, K.A., Agulnick, A.D., Eliazer, S., Kelly, O.G., Kroon, E., Baetge, E.E., 2005. Efficient differentiation of human embryonic stem cells to definitive endoderm. Nat. Biotechnol. 23, 1534–1541.
Dush, M.K., Martin, G.R., 1992. Analysis of mouse Evx genes: Evx-1 displays graded expression in the primitive streak. Dev. Biol. 151, 273–287.
Fuchtbauer, E.M., 1995. Expression of M-twist during postimplantation development of the mouse. Dev. Dyn. 204, 316–322.
Gadue, P., Huber, T.L., Paddison, P.J., Keller, G.M., 2006. Wnt and TGF-beta signaling are required for the induction of an in vitro model of primitive streak formation using embryonic stem cells. Proc. Natl. Acad. Sci. U. S. A. 103, 16806–16811.
Grotewold, L., Plum, M., Dildrop, R., Peters, T., Ruther, U., 2001. Bambi is coexpressed with Bmp-4 during mouse embryogenesis. Mech. Dev. 100, 327–330.
Gurdon, J.B., Bourillot, P.Y., 2001. Morphogen gradient interpretation. Nature 413, 797–803.
Hansson, M., Olesen, D.R., Peterslund, J.M., Engberg, N., Kahn, M., Winzi, M., Klein, T., Maddox-Hyttel, P., Serup, P., 2009. A late requirement for Wnt and FGF signaling during activin-induced formation of foregut endoderm from mouse embryonic stem cells. Dev. Biol. 330, 286–304.
Hoey, T., Levine, M., 1988. Divergent homeo box proteins recognize similar DNA sequences in Drosophila. Nature 332, 858–861.
Imai, Y., Gates, M.A., Melby, A.E., Kimelman, D., Schier, A.F., Talbot, W.S., 2001. The homeobox genes vox and vent are redundant repressors of dorsal fates in zebrafish. Development 128, 2407–2420.
Jones, C.M., Dale, L., Hogan, B.L., Wright, C.V., Smith, J.C., 1996. Bone morphogenetic protein-4 (BMP-4) acts during gastrula stages to cause ventralization of *Xenopus* embryos. Development 122, 1545–1554.
Kanai-Azuma, M., Kanai, Y., Gad, J.M., Tajima, Y., Taya, C., Kurohmaru, M., Sanai, Y., Yonekawa, H., Yazaki, K., Tam, P.P., Hayashi, Y., 2002. Depletion of definitive gut endoderm in Sox17-null mutant mice. Development 129, 2367–2379.
Kawahara, A., Wilm, T., Solnica-Krezel, L., Dawid, I.B., 2000. Antagonistic role of vega1 and bozozok/dharma homeobox genes in organizer formation. Proc. Natl. Acad. Sci. U. S. A. 97, 12121–12126.
Keller, R., Shook, D., 2008. Dynamic determinations: patterning the cell behaviours that close the amphibian blastopore. Philos. Trans. R. Soc. Lond. B. Biol. Sci. 363, 1317–1332.
Khokha, M.K., Yeh, J., Grammer, T.C., Harland, R.M., 2005. Depletion of three BMP antagonists from Spemann's organizer leads to a catastrophic loss of dorsal structures. Dev. Cell 8, 401–411.
Kispert, A., Hermann, B.G., 1993. The Brachyury gene encodes a novel DNA binding protein. EMBO J. 12, 4898–4899.
Kispert, A., Koschorz, B., Herrmann, B.G., 1995. The T protein encoded by Brachyury is a tissue-specific transcription factor. EMBO J. 14, 4763–4772.
Kubo, A., Shinozaki, K., Shannon, J.M., Kouskoff, V., Kennedy, M., Woo, S., Fehling, H.J., Keller, G., 2004. Development of definitive endoderm from embryonic stem cells in culture. Development 131, 1651–1662.
Lane, C.M., Davidson, L., Sheets, M.D., 2004. BMP antagonism by Spemann's organizer regulates rostral–caudal fate of mesoderm. Dev. Biol. 275, 356–374.
Lane, M.C., Sheets, M.D., 2000. Designation of the anterior/posterior axis in pregastrula *Xenopus laevis*. Dev. Biol. 225, 37–58.
Lane, M.C., Sheets, M.D., 2002. Rethinking axial patterning in amphibians. Dev. Dyn. 225, 434–447.
Lane, M.C., Sheets, M.D., 2006. Heading in a new direction: implications of the revised fate map for understanding *Xenopus laevis* development. Dev. Biol. 296, 12–28.
Lane, M.C., Smith, W.C., 1999. The origins of primitive blood in *Xenopus*: implications for axial patterning. Development 126, 423–434.
Latinkic, B.V., Umbhauer, M., Neal, K.A., Lerchner, W., Smith, J.C., Cunliffe, V., 1997. The *Xenopus* Brachyury promoter is activated by FGF and low concentrations of activin and suppressed by high concentrations of activin and by paired-type homeodomain proteins. Genes Dev. 11, 3265–3276.
Maulbecker, C.C., Gruss, P., 1993. The oncogenic potential of deregulated homeobox genes. Cell Growth Differ. 4, 431–441.
McGrath, K.E., Koniski, A.D., Maltby, K.M., McGann, J.K., Palis, J., 1999. Embryonic expression and function of the chemokine SDF-1 and its receptor, CXCR4. Dev. Biol. 213, 442–456.
Melby, A.E., Beach, C., Mullins, M., Kimelman, D., 2000. Patterning the early zebrafish by the opposing actions of bozozok and vox/vent. Dev. Biol. 224, 275–285.
Messenger, N.J., Kabitschke, C., Andrews, R., Grimmer, D., Nunez Miguel, R., Blundell, T.L., Smith, J.C., Wardle, F.C., 2005. Functional specificity of the *Xenopus* T-domain protein Brachyury is conferred by its ability to interact with Smad1. Dev. Cell 8, 599–610.
Moran-Rivard, L., Kagawa, T., Saueressig, H., Gross, M.K., Burrill, J., Goulding, M., 2001. Evx1 is a postmitotic determinant of v0 interneuron identity in the spinal cord. Neuron 29, 385–399.
Moretti, P.A., Davidson, A.J., Baker, E., Lilley, B., Zon, L.I., D'Andrea, R.J., 2001. Molecular cloning of a human Vent-like homeobox gene. Genomics 76, 21–29.
Muyan, M., Boime, I., 1997. Secretion of chorionic gonadotropin from human trophoblasts. Placenta 18, 237–241.
Niehrs, C., Keller, R., Cho, K.W., De Robertis, E.M., 1993. The homeobox gene goosecoid controls cell migration in *Xenopus* embryos. Cell 72, 491–503.
Niehrs, C., Steinbeisser, H., De Robertis, E.M., 1994. Mesodermal patterning by a gradient of the vertebrate homeobox gene goosecoid. Science 263, 817–820.
Nostro, M.C., Cheng, X., Keller, G.M., Gadue, P., 2008. Wnt, activin, and BMP signaling regulate distinct stages in the developmental pathway from embryonic stem cells to blood. Cell Stem Cell 2, 60–71.
Onichtchouk, D., Chen, Y.G., Dosch, R., Gawantka, V., Delius, H., Massague, J., Niehrs, C., 1999. Silencing of TGF-beta signalling by the pseudoreceptor BAMBI. Nature 401, 480–485.
Onichtchouk, D., Glinka, A., Niehrs, C., 1998. Requirement for Xvent-1 and Xvent-2 gene function in dorsoventral patterning of *Xenopus* mesoderm. Development 125, 1447–1456.
Pera, M.F., Andrade, J., Houssami, S., Reubinoff, B., Trounson, A., Stanley, E.G., Ward-van Oostwaard, D., Mummery, C., 2004. Regulation of human embryonic stem cell differentiation by BMP-2 and its antagonist noggin. J. Cell Sci. 117, 1269–1280.
Pevny, L.H., Sockanathan, S., Placzek, M., Lovell-Badge, R., 1998. A role for SOX1 in neural determination. Development 125, 1967–1978.
Pratt, T., Sharp, L., Nichols, J., Price, D.J., Mason, J.O., 2000. Embryonic stem cells and transgenic mice ubiquitously expressing a tau-tagged green fluorescent protein. Dev. Biol. 228, 19–28.
Rashbass, P., Wilson, V., Rosen, B., Beddington, R.S., 1994. Alterations in gene expression during mesoderm formation and axial patterning in Brachyury (T) embryos. Int. J. Dev. Biol. 38, 35–44.
Rivera-Perez, J.A., Mallo, M., Gendron-Maguire, M., Gridley, T., Behringer, R.R., 1995. Goosecoid is not an essential component of the mouse gastrula organizer but is required for craniofacial and rib development. Development 121, 3005–3012.
Rosenberg, L.C., Lafon, M.L., Pedersen, J.K., Yassin, H., Jensen, J.N., Serup, P., Hecksher-Sorensen, J., 2010. The transcriptional activity of Neurog3 affects migration and differentiation of ectopic endocrine cells in chicken endoderm. Dev. Dyn. 239, 1950–1966.
Ruiz i Altaba, A., Choi, T., Melton, D.A., 1991. Expression of the Xhox3 Homeobox Protein in Xenopus Embryos: Blocking Its Early Function Suggests the Requirement of Xhox3 for Normal Posterior Development. Dev. Growth Differ. 33, 651–669.
Ruiz i Altaba, A., Melton, D.A., 1989a. Bimodal and graded expression of the *Xenopus* homeobox gene Xhox3 during embryonic development. Development 106, 173–183.
Ruiz i Altaba, A., Melton, D.A., 1989b. Involvement of the *Xenopus* homeobox gene Xhox3 in pattern formation along the anterior–posterior axis. Cell 57, 317–326.
Sander, V., Reversade, B., De Robertis, E.M., 2007. The opposing homeobox genes Goosecoid and Vent1/2 self-regulate Xenopus patterning. EMBO J. 26, 2955–2965.
Schuldiner, M., Yanuka, O., Itskovitz-Eldor, J., Melton, D.A., Benvenisty, N., 2000. Effects of eight growth factors on the differentiation of cells derived from human embryonic stem cells. Proc. Natl. Acad. Sci. U. S. A. 97, 11307–11312.
Selinummi, J., Seppala, J., Yli-Harja, O., Puhakka, J.A., 2005. Software for quantification of labeled bacteria from digital microscope images by automated image analysis. Biotechniques 39, 859–863.
Showell, C., Binder, O., Conlon, F.L., 2004. T-box genes in early embryogenesis. Dev. Dyn. 229, 201–218.
Steinbeisser, H., Fainsod, A., Niehrs, C., Sasai, Y., De Robertis, E.M., 1995. The role of gsc and BMP-4 in dorsal–ventral patterning of the marginal zone in *Xenopus*: a loss-of-function study using antisense RNA. EMBO J. 14, 5230–5243.
Tada, S., Era, T., Furusawa, C., Sakurai, H., Nishikawa, S., Kinoshita, M., Nakao, K., Chiba, T., 2005. Characterization of mesendoderm: a diverging point of the definitive endoderm and mesoderm in embryonic stem cell differentiation culture. Development 132, 4363–4374.
Wardle, F.C., Papaioannou, V.E., 2008. Teasing out T-box targets in early mesoderm. Curr. Opin. Genet. Dev. 18, 418–425.
Wilkinson, D.G., Bhatt, S., Herrmann, B.G., 1990. Expression pattern of the mouse T gene and its role in mesoderm formation. Nature 343, 657–659.
Wolf, C., Thisse, C., Stoetzel, C., Thisse, B., Gerlinger, P., Perrin-Schmitt, F., 1991. The M-twist gene of Mus is expressed in subsets of mesodermal cells and is closely related to the *Xenopus* X-twi and the *Drosophila* twist genes. Dev. Biol. 143, 363–373.
Wu, Z., Zhang, W., Chen, G., Cheng, L., Liao, J., Jia, N., Gao, Y., Dai, H., Yuan, J., Xiao, L., 2008. Combinatorial signals of activin/nodal and bone morphogenic protein regulate the early lineage segregation of human embryonic stem cells. J. Biol. Chem. 283, 24991–25002.
Xu, R.H., Chen, X., Li, D.S., Li, R., Addicks, G.C., Glennon, C., Zwaka, T.P., Thomson, J.A., 2002. BMP4 initiates human embryonic stem cell differentiation to trophoblast. Nat. Biotechnol. 20, 1261–1264.
Yamada, G., Mansouri, A., Torres, M., Stuart, E.T., Blum, M., Schultz, M., De Robertis, E.M., Gruss, P., 1995. Targeted mutation of the murine goosecoid gene results in craniofacial defects and neonatal death. Development 121, 2917–2922.
Yang, Y.P., Anderson, R.M., Klingensmith, J., 2010. BMP antagonism protects Nodal signaling in the gastrula to promote the tissue interactions underlying mammalian forebrain and craniofacial patterning. Hum. Mol. Genet. 19, 3030–3042.

Yao, S., Chen, S., Clark, J., Hao, E., Beattie, G.M., Hayek, A., Ding, S., 2006. Long-term self-renewal and directed differentiation of human embryonic stem cells in chemically defined conditions. Proc. Natl. Acad. Sci. U. S. A. 103, 6907–6912.

Yasunaga, M., Tada, S., Torikai-Nishikawa, S., Nakano, Y., Okada, M., Jakt, L.M., Nishikawa, S., Chiba, T., Era, T., 2005. Induction and monitoring of definitive and visceral endoderm differentiation of mouse ES cells. Nat. Biotechnol. 23, 1542–1550.

Ying, Q.L., Nichols, J., Chambers, I., Smith, A., 2003. BMP induction of Id proteins suppresses differentiation and sustains embryonic stem cell self-renewal in collaboration with STAT3. Cell 115, 281–292.

Zhang, P., Li, J., Tan, Z., Wang, C., Liu, T., Chen, L., Yong, J., Jiang, W., Sun, X., Du, L., Ding, M., Deng, H., 2008. Short-term BMP-4 treatment initiates mesoderm induction in human embryonic stem cells. Blood 111, 1933–1941.